Journal of Structural Geology, Vol. 9, No. 1, pp. 115 to 119, 1987
Printed in Great Britain

0191-8141/87 $03.00 + 0.00
Pergamon Journals Ltd.

Two-dimensional strain determination by the inverse SURFOR wheel

RENÉE PANOZZO

Geologisches Institut, E.T.H. Zentrum, 8092 Zürich, Switzerland

(*Received* 25 *March* 1986; *accepted in revised form* 2 *June* 1986)

Abstract—A simple method of two-dimensional strain determination from the preferred orientation of deformed lines is presented. It is based on the change of probability of intersecting lines on a given traverse as a function of traverse orientation. The method can be applied to real lines such as grain boundary outlines or to virtual lines such as the tie-lines between centre points of neighbouring grains. In this manner estimates for the strain of surfaces (i.e. of the particles enclosed by the surfaces) and of bulk strain can be obtained.

BASIC CONCEPTS

IF A fabric consisting of randomly oriented surfaces is deformed, the resulting preferred orientation of surfaces carries all the information necessary to derive the finite strain ellipsoid. In the undeformed state, any two-dimensional section displays lines (or outlines) of random orientation. After deformation, the preferred orientation of lines on a given section yields the information necessary to derive the finite strain ellipse (Panozzo 1984).

The method presented here takes the 'inverse' point of view. Rather than considering the actual lines of the fabric and their changes in length and orientation as a function of deformation, the probability of their being intersected on a given traverse is considered. Figure 1(a) shows the undeformed state represented by a set of lines with random orientation. Figure 1(b) shows the same set of lines after deformation. In the undeformed state, the probability of lines being intersected on a given traverse (such as A, B, C or D) is the same for all directions. In other words, within statistical variations, the number of intersections per unit length is constant for all directions.

$$n(\varphi) = N = \text{constant}, \tag{1}$$

where n is the number of intersections per unit length in the undeformed state, and φ is the orientation of the traverse measured with respect to a reference axis x (see Fig. 1a). The average distance between intersection points, d, is inversely related to n:

$$d(\varphi) = 1/n(\varphi) = 1/N = \text{constant}. \tag{2}$$

In Fig. 1(b), the deformed set of lines is shown. On the deformed traverses (A', B', C' and D') the number of intersections has remained the same as before deformation, but because the lengths of the traverses have changed, so have the average distances between points of intersection. The deformed length, L', in a given direction is given by:

$$L'(\phi') = \sqrt{\lambda} = 1/\sqrt{(1/\lambda_1 \cdot \cos^2(\phi') + 1/\lambda_2 \cdot \sin^2(\phi'))}, \tag{3}$$

where ϕ' is the angle between the direction of length L' in the deformed state and the direction of $\lambda_1 \cdot \lambda$ is the quadratic extension; $\sqrt{\lambda_1}$ and $\sqrt{\lambda_2}$ are the principal axes of the strain ellipse. Note that ϕ' is not equal to φ'; they are the same only if λ_1 is parallel to the reference axis x'. In the general case, the strain ellipse is inclined at an angle, φ_i (see Fig. 2), and

$$L'(\phi') = L'(\varphi' - \varphi_i). \tag{4}$$

The average distance between intersections after deformation is given by

$$d'(\varphi') = L'(\varphi' - \varphi_i) \cdot d(\varphi), \tag{5}$$

and the number of intersections per unit length in the deformed state varies as the inverse of the length change in that direction:

$$n'(\varphi') = 1/d'(\varphi'). \tag{6}$$

Substituting for $d'(\varphi')$ (equation 5) and then for $L'(\varphi' - \varphi_i)$ (equation 3) and $d(\varphi)$ (equation 2), one finds

$$n'(\varphi') = N \cdot \sqrt{(\lambda_1' \cdot \cos^2(\varphi' - \varphi_i) + \lambda_2' \cdot \sin^2(\varphi' - \varphi_i))}, \tag{7}$$

where $\sqrt{\lambda_1'}$ and $\sqrt{\lambda_2'}$ are the reciprocal principal elongations. The function $n'(\varphi')$, relating the number of intersections n' in the deformed state to the orientation φ' of the traverse, is essentially determined by the equation of the reciprocal strain ellipse since N, the number of intersections on a traverse in the undeformed state, and φ_i, the orientation of the long axis of the strain ellipse with respect to the x' direction, are both constants.

The function $n'(\varphi')$ exhibits one maximum ($n'(\varphi')_{max} = N \cdot \sqrt{\lambda_2'}$) at $\varphi'_{max} = 90° + \varphi_i$ and a minimum ($n'(\varphi')_{min} = N \cdot \sqrt{\lambda_1'}$) at $\varphi'_{min} = \varphi_i$. Therefore, if the curve $n'(\varphi')$ of a given fabric has been determined, the axial ratio, $\sqrt{\lambda_2}/\sqrt{\lambda_1}$, of the strain ellipse and the orientation, φ_i, of its long axis can be derived.

$$\sqrt{\lambda_2}/\sqrt{\lambda_1} = \sqrt{\lambda_1'}/\sqrt{\lambda_2'} = n'(\varphi')_{min}/n'(\varphi')_{max}, \tag{8a}$$

$$\varphi_i = \varphi'_{min}. \tag{8b}$$

In Fig. 1(b), $n'(\varphi')_{min}/n'(\varphi')_{max} = \sqrt{\lambda_2}/\sqrt{\lambda_1} = 0.5$ and

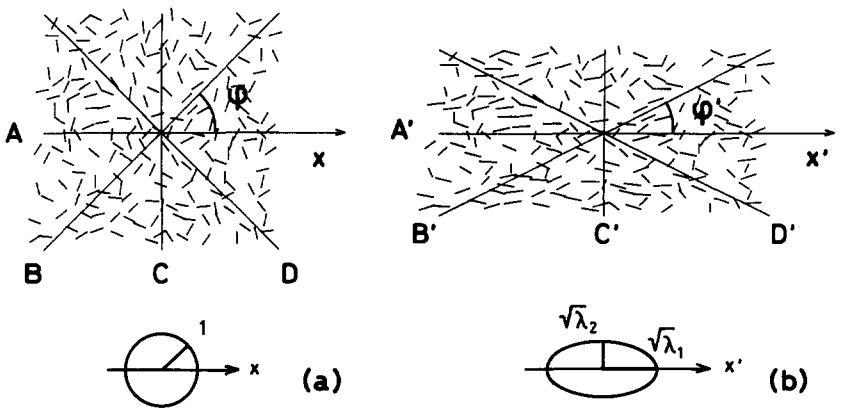

Fig. 1. (a) Set of random lines and traverses in the undeformed state. (b) The same lines after deformation. Axial ratio of strain ellipse, $b/a = 0.5$, quadratic extensions, $\sqrt{\lambda_1} = 1.414$, $\sqrt{\lambda_2} = 0.707$. x and x' = axes of reference in the undeformed and deformed states, respectively, φ and φ' = angles of orientation of traverses in the undeformed and deformed states respectively.

the orientation of the long axis of the strain ellipse with respect to the reference direction (i.e. the orientation, φ'_{min}, where $n'(\varphi')_{min}$ occurs) is 0°.

The proposed method of strain analysis consists of rotating a set of parallel lines of fixed and constant length through 180° and counting the intersections with the lines (or outlines) of the deformed fabric at regular intervals of φ'. [The name of the method is derived from another method of strain determination that considers SURFace ORientations (Panozzo 1984).]

METHOD

Figure 3 shows the inverse SURFOR wheel in the starting position. This figure may also be used to create copies of the wheel on transparent film.

The procedure is as follows:

(1) On the drawing of the fabric outlines (i.e. of the lines that are assumed to have been randomly oriented in the undeformed state) a reference direction, x', and a centre point, C, are chosen (see Fig. 4a). The centre of the inverse SURFOR wheel is placed on C, the set of parallel lines on the wheel in the direction of x'.

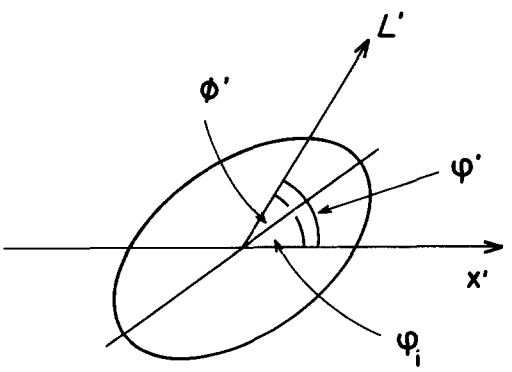

Fig. 2. General orientation of a line, L', and the strain ellipse with respect to a reference direction, x'. φ_i = orientation of the long axis of the strain ellipse with respect to x'; φ' = orientation of the line with respect to x'; ϕ' = orientation of the line with respect to the long axis of the strain ellipse in the deformed state.

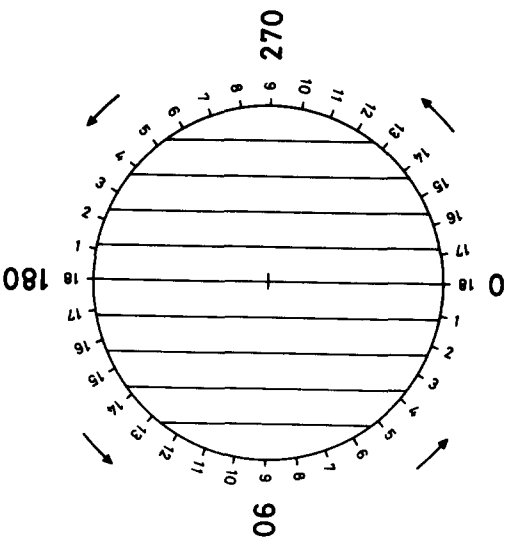

Fig. 3. The inverse SURFOR wheel.

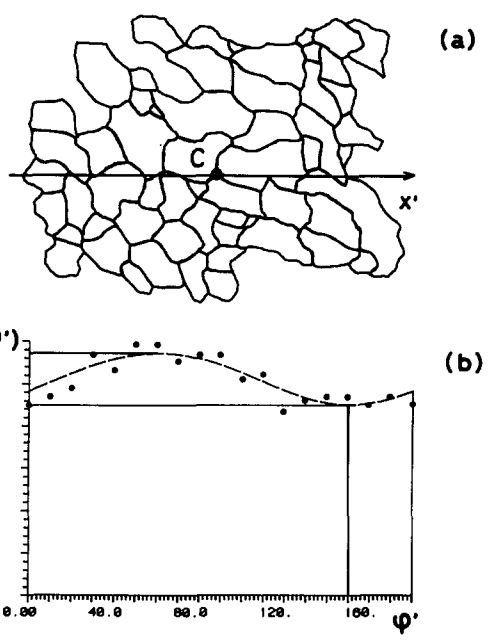

Fig. 4. (a) Outlines of grain boundaries in a quartzite (after fig. 7.16, p. 118 of Ramsay & Huber 1983); x' = reference direction, C = centre. (b) Analysis of the grain boundaries shown in (a); plot of number of intersections, n', versus orientation, φ'; dashed line = curve fitted through points. $n'(\varphi')_{min} = 45$, $n'(\varphi')_{max} = 57$.

(2) The number of intersections of the set of parallel lines with the fabric outlines is counted for 18 orientations, turning the wheel counterclockwise as indicated by the arrows. Position 1 corresponds to an angle of 10°, position 2 to 20°, etc. The number of intersections, n', are plotted as a function of the orientation, φ' (see Fig. 4b), measuring the angles counterclockwise. The number of intersections per orientation should average 50 or more. Division by the total length, L, of the set of test lines (in order to obtain the number of intersections per unit length) is not necessary, as L is a constant.

(3) A curve is fitted through the points. This can be done (a) by 'eye-balling' or (b) by calculating a best-fit curve. The minimum and maximum values, $n'(\varphi')_{min}$ and $n'(\varphi')_{max}$, of the curve and the angle, φ'_{min}, at which the minimum occurs are determined. The ratio $n'(\varphi')_{min}/n'(\varphi')_{max}$ is the ratio, $\sqrt{\lambda_2}/\sqrt{\lambda_1}$, of the strain ellipse, the angle φ'_{min} is the orientation φ_i of its long axis.

APPLICATION

The fabric shown in Fig. 4(a) has been analyzed using three different techniques:

(a) using the method of Fry (1979), as described in Ramsay & Huber (1983, p. 117–124);
(b) using the regular SURFOR method (Panozzo 1984);
(c) using the inverse SURFOR wheel presented in this paper.

The advantages of methods (a) and (c) are ease of application and the fact that all necessary calculations can be done by hand. In both cases it only takes a relatively short time (depending on the size of the analyzed area) to obtain the primary plot. The critical step in method (a) is fitting an ellipse into the vacancy field left between the point clusters. The critical step in the method presented here is fitting a smooth curve through the points of the n'/φ' plot (see Fig. 4b). Method (b) is computer-based and uses the projections of particle outlines. It involves digitization of particle contours on enlarged photographs. In testing and practical applications this method has proved to be very sensitive, while yielding reliable results.

The results obtained by the three methods are presented in Table 1. The axial ratios obtained from the regular SURFOR method (b) and the inverse SURFOR wheel (c) are practically the same. The orientations of the long axis of the strain ellipse are also quite similar considering that the angular interval at which $n'(\varphi')$ is evaluated is 10°. The axial ratio obtained by Fry's method (a) is greater than the ratio obtained by the other two methods. The angle, φ_i, between the long axis of the strain ellipse and the reference direction, x', obtained using Fry's method, deviates from the one obtained by the SURFOR method by 7°.

It should be noted that the two different types of analysis do not make use of the same fabric element. Fry's method is based on change of distance between the centre points of neighbouring grains, while the SURFOR methods are based on the deformation of grain boundary surfaces. The bulk deformation determined by Fry's method and the deformation of the grain boundary surfaces measured by the SURFOR methods need not coincide, and thus different results may be obtained using these two methods. This would be the case, for example, if there were a competence contrast between particles and matrix (see Discussion).

In order to better compare Fry's method and the inverse SURFOR wheel, another application of the latter is used. It is assumed that the undeformed state is defined by the random orientation of the (virtual) tie-lines between the centre points of neighbouring grains (see Fig. 5a) rather than by the random orientation of the (real) grain boundary outlines (Fig. 4a). This is equivalent to assuming that the distribution of centre points of the undeformed fabric is isotropic anticlustered (i.e. Fry's original assumption).

The centre points of the fabric shown in Fig. 4(a) have been determined by inspection and the tie-lines between them drawn in by hand. The curve resulting from the analysis of the deformed tie-lines is shown in Fig. 5(b), and the values of the derived strain parameters are given in Table 1 [method (d)]. The values for both the axial ratio $\sqrt{\lambda_2}/\sqrt{\lambda_1}$ and the orientation of the long axis of the strain ellipse are now close to the values determined by the regular SURFOR method. In other words, the bulk strain and the strain recorded in the grain boundaries are probably the same. It is therefore assumed that the difference between the results obtained using Fry's method and those obtained using the inverse SURFOR wheel is an artefact of the different measuring techniques. It is introduced during the critical step of each method; that is during ellipse fitting in the first case and curve fitting in the second. In the discussion by Ramsay & Huber (1983, p. 124), the ambiguity associated with fitting an ellipse to Fry's primary plot is clearly recognized.

Table 1. Results of fabric analysis

Method	Analyzed fabric element	Axial ratio of strain ellipse $\sqrt{\lambda_2}/\sqrt{\lambda_1}$	$\sqrt{\lambda_1}/\sqrt{\lambda_2}$	Orientation of long axis φ_i
(a) Fry	Centre points	0.63	1.59	152°
(b) SURFOR	Outlines	0.78	1.28	145°
(c) Inverse SURFOR	Outlines	0.79*	1.27	150°*
(d) Inverse SURFOR	Tie-lines	0.73†	1.37	150°†

*See Fig. 4(b).
†See Fig. 5(b).

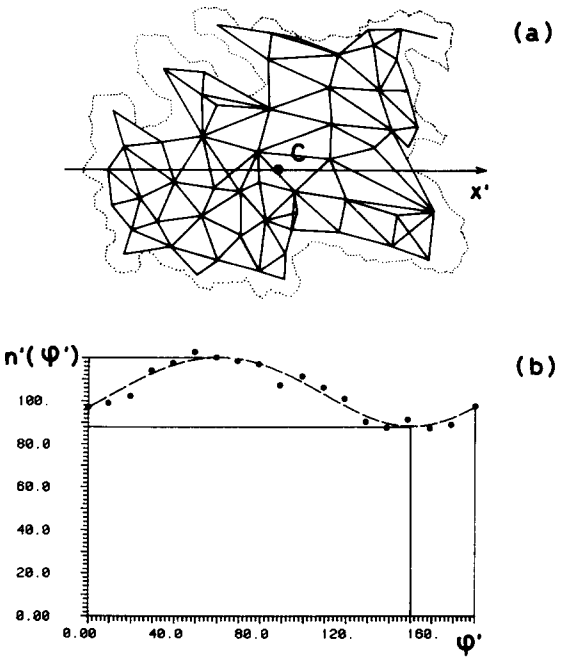

Fig. 5. (a) Fabric consisting of tie-lines between centre points of neighbouring grains: x' = reference direction, C = centre. (b) Analysis of the tie-lines shown in (a): plot of points of intersection, n', versus orientation, φ'; dashed line = curve fitted through points. $n'(\varphi')_{min} = 88$, $n'(\varphi')_{max} = 120$.

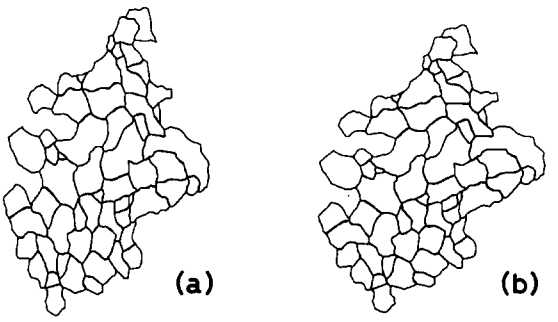

Fig. 6. Reversed strain of the fabric shown in Fig. 4(a), (a) using the strain values obtained by Fry's method, (b) using the strain values obtained by the SURFOR method.

DISCUSSION

A few general points associated with the interpretation of fabrics in terms of strain are addressed below.

1. The initial state

In the example analyzed above, as in most other cases, the initial state is unknown. Random orientation of surfaces and random anticlustered distribution of centre points are assumed for the initial state (cf. Fry 1979, Panozzo 1984). One may well argue that, for example, sedimentation and lithification must have introduced a pretectonic fabric and that the value obtained from fabric analysis should be corrected accordingly. However, this correction cannot be applied because information concerning the pretectonic fabric is not available.

It should be noted that making certain assumptions concerning the initial state is by no means unique to the method described here. The advantage of the method, however, is that it provides a quick measurement of both the strain recorded in the centre point distribution and the strain recorded in the grain boundary surfaces. If they coincide, the above-mentioned assumption concerning the initial state can be sustained. If they differ, the initial state has to be redefined as *either* a state of random distribution of centre points *or* a state of random orientation of surfaces. Another possible way of explaining the divergence would be to assume strain partitioning (see below).

2. Deformational behaviour of grain boundaries

The second assumption on which strain interpretation relies is that the net effect of all active deformation processes be such that the grain boundaries can be regarded as passive markers. This is the case, for example, for crystal-plastic deformation mechanisms. It is not the case for grain boundary migration, pressure solution, recrystallization, or other deformation mechanisms in which the behaviour of grain boundaries (i.e. of surfaces) is independent of the behaviour of the grains (i.e. of volumes).

For the sample analyzed here (which is a Cambrian quartzite deformed at conditions of relatively low pressure and temperature) it was assumed that grain boundaries acted as passive markers. A qualitative test for this assumption consists of numerically reversing the strain of the sample by the amount determined from surface analysis. If, after reversing the strain, the grain boundaries appear randomly oriented (having a uniform orientation distribution of surface), if the grains are more or less isometric (giving the fabric a natural undeformed look), and if the centre point distribution is isotropic, the grain boundaries may be interpreted as passive markers. Note that this is merely an empirical inference which implies that the strain recorded in the grain boundary surface is equal to the bulk strain, and that the bulk strain is given by the centre point distribution.

The fabric shown in Fig. 4(a) has been undeformed using the strains obtained by Fry's method and the SURFOR method (see Figs. 6a & b, respectively). Inspection and additional strain analysis of these fabrics by other, independent, methods (R_f/φ-method (Ramsay 1967), and particle orientation (Panozzo 1983)) show that Fig. 6(b) represents an undeformed fabric whereas Fig. 6(a) appears strained. It is therefore concluded that the strain obtained by applying the inverse SURFOR wheel to the tie-line fabric represents a better estimate of the bulk strain than the one obtained from using Fry's method.

The general question as to whether grain boundary outlines of (monomineralic) crystalline rocks may be used as strain markers is not unique to the method described here. Because of the possibility of grain boundary migration, recrystallization, grain boundary sliding, etc., it seems obvious that they are less reliable than the outlines of fossils or of particles in a matrix.

If the method is applied to particle surfaces which are completely convex (or if the indentations display no

preferred orientation that is different from the preferred orientation of the particles), the strain determined from the particle outlines is equal to the strain determined from the shape of the cross-sectional areas of the particles (see Panozzo 1984). In these cases, surface strain and volume strain (of particles) coincide. The advantage of this is that surface strain analysis can be substituted for the analysis of grain shapes. This may lead to less biased results because one can avoid approximating grain shapes by ellipses, finding long and short axes, etc.

3. *Strain partitioning*

As has been mentioned, the strain recorded in the change of distance between neighbouring grains and that recorded in the change of length and orientation of grain boundary surfaces need not coincide. One cause for such differences may be the fact that surfaces do not act as passive markers and hence do not really record strain (see above). Another possible explanation has been mentioned, which arises from mechanical considerations. If the rheologies of particles and matrix are different from one another, different amounts of strain are recorded. In this case the particle surfaces do actually record strain and, given the material properties and the appropriate theory, the bulk strain can be determined from them (e.g. Gay 1968).

In polymineralic rocks strain partitioning between the different phases may occur. In monomineralic rocks strain partitioning between grain volumes and grain boundary surfaces may occur: if the grains are not perfectly welded, a certain amount of strain may be taken up along the grain boundaries by grain boundary sliding. Another possibility is the formation of a core–mantle structure where deformation is restricted to the mantle region of grains.

The method described here does not require complete grain boundary outlines. One is therefore capable of analyzing disconnected surface elements, provided only that their initial orientation was random and that they respond to deformation as passive markers. Thus, one may analyze in separate turns the deformational behaviour of different mineral surfaces or of selected mineral interfaces or reaction surfaces. This is very useful in cases where strain partitioning is to be expected not only between different phases but also between different portions of a grain boundary surface, or disconnected surface elements.

It should be noted that the method is also valid if the outlines are truncated by the limits of the sampling area (always assuming that the initial orientation of the lines was random and that the present preferred orientation is due to deformation).

4. *Fabric versus strain*

The rock geometry, that is the fabric and the inferred deformation have to be distinguished carefully. Not every preferred orientation of surface is due to deformation, in fact many are not even compatible with an interpretation of strain.

For randomly oriented surfaces the orientation distribution function is uniform. Its characteristic shape is the circle (Panozzo 1986); the corresponding n'/φ' plot is a constant. After deformation, and given the above mentioned conditions, the n'/φ' plot corresponds to that of the finite strain ellipse. The theoretical function $n'(\varphi')$ is given in equation (7). Within an interval of 180°, this is a unimodal symmetric function. Whether deviations of measured data from this theoretical form are statistically significant or not is hard to assess. So far, the following procedure has been adopted: if the function is unimodal and symmetric (i.e. $\alpha_{max} - \alpha_{min} = 90° \pm 5°$), the characteristic shape is taken to be an ellipse and an interpretation in terms of strain cannot be excluded on the basis of the shape of the function $n'(\varphi')$. In other words, this method represents an independent test whether a given preferred orientation is at all compatible with an interpretation in terms of strain or not.

CONCLUSIONS

The method of the inverse SURFOR wheel is a valid and practical tool for fabric analysis. It is easy to use and does not require computer facilities. The results obtained from applying it to real surfaces compare well with those from the regular SURFOR method. Interpretation in terms of strain rests on the assumption that the strain is recorded in the preferred orientation of surfaces (e.g. grain boundary outlines).

The method may also be applied to tie-lines between centre points of neighbouring particles. This is equivalent to assuming that in the undeformed state the orientations of the (virtual) tie-lines are random, that is, the distribution of centre points is isotropic and anticlustered. The method then compares favourably with Fry's method, since there appears to be less ambiguity associated with fitting a curve to the n'/φ' plot than with fitting an ellipse into the vacancy field of the Fry plot.

Acknowledgements—I am grateful to the reviewers, C. C. Ferguson and P.-Y. F. Robin, for stimulating criticism.

REFERENCES

Fry, N. 1979. Random point distribution and strain measurements. *Tectonophysics* **60**, 89–105.

Gay, N. C. 1968. Pure shear and simple shear deformation of inhomogeneous viscous fluids. 2. The determination of the total finite strain in a rock from objects such as deformed pebbles. *Tectonophysics* **5**, 295–302.

Panozzo, R. 1983. Two-dimensional analysis of shape fabric using projections of lines in a plane. *Tectonophysics* **95**, 279–294.

Panozzo, R. 1984. Two-dimensional strain from the orientation of lines in a plane. *J. Struct. Geol.* **6**, 215–221.

Panozzo, R. 1986. Grain boundary surface orientation as indicator of strain and deformation mechanisms in shear zones (Abstract). Shear Criteria Meeting, 22–24 May 1986, Imperial College, London.

Ramsay, J. G. 1967. *Folding and Fracturing of Rocks*. McGraw-Hill, New York.

Ramsay, J. G. & Huber, M. I. 1983. *The Techniques of Modern Structural Geological, Vol. 1: Strain Analysis*. Academic Press, London.